Changes in the absorption and scattering properties in the Near-infrared region during the growth of *Bacillus subtilis* in liquid culture

Elitsa Dzhongova[1], Colin R. Harwood[2], Suresh N. Thennadil[1*+]

[1]School of Chemical Engineering and Advanced Materials, and [2]Institute for Cell and Molecular Biosciences, Newcastle University, Newcastle upon Tyne, United Kingdom

[+]Current Address: Department of Chemical and Process Engineering, University of Strathclyde, Glasgow, United Kingdom

* Correspondence to Suresh N. Thennadil. Email: suresh.thennadil@strath.ac.uk

ABSTRACT

Multiple scattering of light by cells poses a significant challenge in the development of NIR-based methodologies to reliably extract chemical and physical information contained in the spectra collected during the bacterial growth cycle. The extent of information that can be obtained from NIR spectra could, in principle, be vastly improved if the scattering and absorption effects can be effectively separated. This study focuses on the methodology for extracting the bulk optical properties over the course of the bacterial growth cycle and investigates the nature and extent of changes in the optical properties with time. By inverting the Radiative Transfer Equation (RTE) using 3 measurements viz. total diffuse reflectance, total diffuse transmittance and collimated transmittance, the bulk absorption coefficient (μ_a), the bulk scattering coefficient (μ_s) and the anisotropy factor (g) are extracted and their changes during the course of the growth cycle are investigated. In this study, a simple bacterial growth system consisting of *Bacillus subtilis* growing in an aqueous solution (minimum medium) was investigated. The changes in the optical properties of this system during bacterial growth, stationary and decline phases were investigated by inverting the measurements using the adding-doubling method to solve the RTE, in the wavelength region of 950nm – 1850nm. This study shows that during growth in liquid culture, the absorption and scattering property changes can be consistently extracted from measurements under multiple light scattering conditions. The estimation of anisotropy factor was not reliable beyond 1200nm at low bacterial cell counts, but reliability increased with increasing biomass concentration. At all stages in the growth cycle, the anisotropy factor could not be reliably extracted in the

first overtone region. However this does not appear to adversely affect the estimation of the absorption and scattering coefficients.

Keywords: Multiple light scattering, optical properties, radiative transfer theory, fermentation, *Bacillus subtilis*.

INTRODUCTION

During the last two decades, there has been considerable interest in utilising near-infrared (NIR) spectroscopy for monitoring microbial fermentation processes, since this technique has the potential to provide information about both the chemical and physical state of a system. The fact that NIR measurements could be made with minimum or no-sample preparation, coupled with the availability of robust, easy to operate instruments with high signal-to-noise characteristics, has made this technique a promising tool for at-line and on-line for monitoring of microbial growth [1, 2].

Several research groups have investigated the utility of NIR spectroscopy on various fermentation processes such as wine[3] and beer[4], fermentation, and batch, fed-batch and continuous cultivations[5-8] in combination with chemometric techniques. Multiple scattering of light by the cells poses a significant challenge in the development of NIR-based methodologies to extract reliable chemical and physical information contained in the spectra of growing suspension of microbial cells. The extent of information that can be obtained from NIR spectra could, in principle, be vastly improved if the scattering and absorption effects can be effectively separated.

In this paper, we investigate an approach to separate the absorption and scattering effects using the Radiative Transfer Equation (RTE) to account for multiple scattering of light[9, 10]. By inverting the RTE, the bulk transport coefficients *i.e.* the bulk absorption (μ_a) and scattering (μ_s) coefficients and the anisotropy factor (g), can be extracted. The changes in the absorption and scattering properties can then be separately monitored during the microbial growth cycle. The bulk scattering coefficient will be pre-dominantly related to changes in properties such as cell size, and biomass concentration whereas information regarding non-scattering constituents such as glucose, and product concentrations will be contained in the bulk absorption coefficient. Thus by extracting μ_a and μ_s, it may be possible to obtain more information for monitoring microbial growth than could be obtained using only the transmittance or reflectance data. This is because the μ_a and μ_s data discriminates better between variations in the constituents of the cells and growth medium by taking advantage of the different information content of the two coefficients. Further, from the point of view of building calibration models for estimating the concentrations of product and nutrients, the removal of the confounding effects due to multiple light scattering from the absorption effects could lead to simpler and more robust models.

As a first step towards achieving reliable models for predicting the concentrations of components in a culture medium by separating the absorption and scattering effects, this study focuses on the methodology for extracting the bulk optical properties and investigates the nature and extent of changes in the optical properties over the course of a

bacterial growth cycles. For this purpose a simple culture system was established consisting of *Bacillus subtilis* growing in an aqueous solution (minimum medium). The changes in the optical properties of this system during growth, stationary and decline phase were studied using measurements in the wavelength region of 950nm – 1850nm.

MATERIALS AND METHODS

A. Inversion of the RTE to extract optical properties

The Radiative Transfer Equation (RTE) which describes the transport of light through a medium containing particles is give by [9],

$$\frac{dI(\lambda,\vec{r},\hat{s})}{ds} = -\mu_t(\lambda)I(\lambda,\vec{r},\hat{s}) + \frac{\mu_t(\lambda)I(\lambda,\vec{r},\hat{s})}{4\pi}\int_{4\pi}p(\hat{s},\hat{s}')I(\lambda,\vec{r},\hat{s}')d\omega' \qquad (1)$$

where $I(\lambda,\vec{r},\hat{s})$ is the specific intensity of light of wavelength λ at point $\vec{r}$ with radiation incident along direction $\hat{s}$, $\mu_t(\lambda)$ $[=\mu_s(\lambda)+\mu_a(\lambda)]$ is the bulk extinction coefficient, $\mu_s(mm^{-1})$ is the bulk scattering coefficient and μ_a (mm^{-1}) is the bulk absorption coefficient and $p(\hat{s},\hat{s}')$ is the phase function which is a measure of the angular distribution of scattered light and is usually approximated as a function of the anisotropy factor g. The bulk scattering and absorption coefficients are related to the individual species *i* present in a sample as follows:

$$\mu_a(\lambda) = \sum \rho_i \sigma_{a,i}(\lambda) \qquad (2)$$

and

$$\mu_s(\lambda) = \sum \rho_i \sigma_{s,i}(\lambda) \qquad (3)$$

where ρ_i is the number density (concentration) of species *i*, $\sigma_{a,i}$ and $\sigma_{s,i}$ are the absorption and scattering cross-sections respectively of species *i*. The phase function is usually approximated as a function of the scattering angle θ and anisotropy factor g (= $\langle\cos\theta\rangle$). One of the widely used functions is the Henyey-Greenstein approximation[9-11]

$$p(\cos\theta) = 0.5(1-g^2)(1-g^2+2\cos\theta)^{1.5} \quad (4)$$

Thus, for describing the propagation of light of wavelength λ through a suspension using (1) along with appropriate boundary conditions, the 3 transport parameters viz. μ_a, μ_s and g are needed. In the context of the inverse problem, this means that the information content of the suspension is contained in these 3 parameters and to extract the parameters, at least 3 measurements have to be made at each wavelength. The absorption (μ_a) and scattering (μ_s) parameters are of particular interest since they are sensitive to changes in the physical and chemical state of the suspension.

In this study, the optical parameters were extracted using an inversion method based on the adding-doubling method for numerically solving the RTE including the boundary effects due to the glass cuvette[11-13]. In the adding-doubling method, the total diffuse reflectance (R_d) and total diffuse transmittance (T_d) from a very thin layer having the same optical properties as the sample is calculated using for example the single scattering theory or the diamond-initialization method[12,14]. It has been shown that the diamond initialization method is more accurate than using the single scattering theory[14] and therefore the former was used in this work. Once T_d and R_d for the initial thin layer has been calculated, the values for a layer double the thickness can be obtained

by invoking the principle of invariance[10]. This process of doubling the layers is continued until the desired thickness (i.e. the sample thickenss) is reached. Since in this work the sample is placed in a glass cuvette, the (specular) reflection and transmission at the air-glass and the glass-sample boundaries have to be taken into account. This is done by first computing the reflectance and transmittance from the glass and then as before invoking the principle of variance to "add" the sample and glass layers to obtain the total diffuse reflectance and transmittance from the entire glass-sample-glass entity. The calculation of the collimated transmission is straightforward and is given by Beer's law:

$$T_c(\lambda) = \exp(-\mu_t(\lambda)\ell) \qquad (5)$$

where $\mu_t(\lambda)$ is the bulk extinction coefficient and ℓ is the sample thickness (i.e. the cuvette pathlength). The mathematical and the implementation details of the adding-doubling method can be found in the literature cited[10-14].

To use the adding-doubling method as part of an inversion scheme to extract the bulk absorption and scattering properties,, the 3 measurements needed are the total diffuse transmittance (T_d), total diffuse reflectance (R_d) and collimated transmittance (T_c). The total diffuse transmittance and reflectance measurements are obtained using an integrating sphere set-up. It should be noted that the total diffuse transmittance includes the collimated portion of the transmitted light and the total diffuse reflectance includes the specular reflectance from the boundaries. These are taken into account in the adding-doubling calculations. Due to the correlation between T_d and T_c measurements, there is an inherent instability in the inversion which could lead to problems with convergence

under some circumstances such as when the absorbance is very high. A schematic of the three measurement configurations is shown in figure 1.

In addition to the three measurements, to invert the RTE for the system (glass-suspension-glass) using the adding-doubling method, the refractive index of the glass cuvette and the suspension are required as inputs. The refractive index of the glass cuvette was taken to be 1.523 (given by the manufacturer). The refractive index of the sample was taken as the average refractive index, 1.3362 estimated by measuring the refractive index of several samples with a refractometer.

The inversion algorithm starts by taking as inputs the refractive index of sample and glass and the thickness of the sample i.e. the cuvette pathlength (ℓ). In addition, initial guess values of the bulk absorption albedo (α), optical depth (τ) the anisotropy factor (g_o) of the sample have to be provided. The albedo and the optical depth are given by:

$$\alpha = \frac{\mu_s}{(\mu_s + \mu_a)} \text{ and } \tau = (\mu_s + \mu_a)\ell \qquad (6)$$

The reason for using the albedo and optical depth as the parameters for the inversion instead of directly using μ_a and μ_s is because the algorithm is much more stable when the former two parameters are used. Further the adding-doubling equations are naturally cast in terms of albedo and optical depth and once these are extracted the scattering and absorption parameters can be obtained using (6). The calculated total diffuse reflectance (R_{dcalc}), total diffuse transmittance (T_{dcalc}) obtained from the adding-doubling routine and the collimated transmittance obtained from using Beer's law (T_{ccalc})

for the input guess values of albedo and optical depth are then compared with the corresponding measured values:

$$\xi = \text{abs}(R_d - R_{dcalc}) + \text{abs}(T_d + T_{dcalc}) + \text{abs}(T_c - T_{ccalc}) \quad (7)$$

The guess values are then updated and the iterations carried out until convergence ($\xi \leq 1.0e-7$) is achieved. This iteration was carried out using the function "fmincon" of the MATLAB® Optimization toolbox to minimize (7).

B. Experimental details

The growth studies were conducted using the Gram-positive bacterium *Bacillus subtilis* strain 168 which was obtained from the Institut Pasteur, Paris. The strain was cultivated in 100ml Spizizen's minimal medium and trace element solution[15] in a 250 ml Erlenmeyer flask. For all the bacterial growth cycle experiments were carried out with the culture at an initial pH of 7 ± 0.5. The temperature was controlled during the entire bacterial growth cycle at 37^{0}C±0.5, and agitation rate set at 220rpm. In this study, data from the growth, stationary and decline phases were collected from separate cultivations. A total of 9 growth cycles were performed. For the first 3 cultures, data was collected during the growth phase. For cultures 4-6, data was collected only during the stationary phase and for cultures 7-9, data was collected during the decline phase. Since all the growth cycle runs were performed under the same conditions, each of the set of three runs for each phase (growth, stationary and decline) are essentially replicate runs. For all these cultures, during the data collection phase, a total of five samples were taken at approximately 2 hour intervals. The progress of the cultivations was also followed by making optical density measurements which provided information regarding the stage of

the growth cycle which, in turn, ensured that the samples were collected at the appropriate growth phase. All measurements for optical density were made using a CARY 5000 UV-Vis NIR spectrophotometer in absorption mode at a 600nm wavelength with a 1cm path length cuvette.

On each sample the following spectroscopic measurements were made: Total diffuse reflectance (R_d), total diffuse transmittance (T_d) and collimated transmittance (T_c). These measurements were made using a UV-Vis-NIR spectrophotometer (Cary 5000, Varian Scientific Instruments) equipped with an integrating sphere (Diffuse Reflectance Accessory - DRA 2500) by placing the samples in a special optical glass cuvette with path length of 4mm. The measurements were made over the wavelength range of 950nm - 1850nm with an average integration time of 0.4s, an average signal band-width of about 15nm and wavelength interval 4nm.

For these samples, biomass was measured gravimetrically. Aliquots of 5ml suspension were filtered without washing through pre-weighed Millipore filter (pore size 0.45μm). After the culture suspension was filtered, the filters were then dried at 50^{o}C to a constant weight, cooled down in a vacuum desiccator, and then weighed again. The difference between the dried and pre-weighed filter was expressed as weight of the dry cells per sample volume.

RESULTS AND DISCUSSION

Figure 2 shows the optical density curves during the cultivation for the different phases and the points on the curves indicate when the samples for measurements were

drawn from the flask. While the same recipe was used for all the cultivations, it is seen that for the 3 runs in each of the growth phases, there are small but distinctive variations in the optical density curves and the points where the samples were drawn are not exactly at the same time point on the curves.

Figures 3(a)-(c) show the raw spectra plotted in absorbance units, of the samples collected during all the cultivations using the different measurement configurations viz. Total diffuse reflectance (R_d), total diffuse transmittance (T_d) and collimated transmittance (T_c). Both T_c and T_d are noisy around the 1450nm water absorption peak (Figures 3 b and c). In the case of R_d, the spectra appear to flatten out beyond 1400nm. The reason is that in this region, the amount of light reflected from the sample is small compared to the specular reflectance contribution from the glass cuvette. However, the information regarding changes in the sample is embedded in the spectrum and can be extracted by accounting for the specular reflectance as is done when extracting the optical properties.

The extracted optical properties viz. bulk scattering coefficient $\mu_s(\lambda)$, bulk absorption coefficient $\mu_a(\lambda)$ and anisotropy factor $g(\lambda)$ for the samples collected during the growth phase are shown in Figures 4(a)-(c). In these plots, the gaps in the wavelength region 1360-1550nm are because the inversion using the adding-doubling method does not converge due to the high absorbance in this region. To obtain the optical properties in this region, sample thickness would have to be reduced by using cuvettes with path lengths smaller than 4mm. It can be seen that the relative change in $\mu_s(\lambda)$ is high compared to the relative changes in $\mu_a(\lambda)$ over the duration of the growth phase. This is

expected since, in the cultivation system considered here, the largest variation is due to the increase in biomass. While the biomass also affects $\mu_a(\lambda)$, the absorption due to biomass in the NIR region is small compared to the absorption due to water, therefore the relative changes due to an increase in biomass is small.

The extracted anisotropy factor also exhibits changes during the growth phase. In the early stage of the growth phase, across the wavelength region 950-1350nm, $g(\lambda)$ drops sharply towards zero beyond 1200nm or flattens out in this region. This is physically inconsistent. It is noticed that the wavelength beyond which it falls in this manner increases as the growth cycle progresses. It could be concluded that this effect is due to the fact that the low biomass in the initial stages of the cultivation and the resulting low scattering which characteristically falls off at higher wavelengths could be a factor in the inversion not being effective in extracting the anisotropy factor under such conditions. This effect has previously been evidenced in polystyrene-water system[12] where a sample with 0.15% of polystyrene particles by weight was considered. In that study it was shown that while the estimated values of anisotropy factor was unreliable in the region where it falls off sharply, it did not affect the estimation of $\mu_a(\lambda)$ and $\mu_s(\lambda)$. As the growth cycle progresses, the estimates of $g(\lambda)$ become stable over a larger span of wavelengths. Beyond 1500nm, $g(\lambda)$ stays around 0.8 which is the initial guess value input to the inverse adding-doubling program and thus cannot be expected to be a reliable estimate. Changing the initial guess values (0.7 and 0.9 were tried) resulted in $g(\lambda)$ over this wavelength range to converge to a value close to those guess values, thus reinforcing the conclusion that the estimate of the anisotropy factor in this region is not reliable

though this does not affect the estimation of the bulk absorption and scattering coefficients.

Examining figure 4, it can be seen that the extracted optical properties are consistent over the three cultivations for the growth stage. Since the samples were taken at approximately the same point in the growth cycle during each of the three cultivations which all used the same culture medium and analytical protocol, we would expect, if the inversion method is stable, to obtain similar optical properties at these time points. The optical properties corresponding to similar time points are indeed similar. The small differences in the magnitude can be attributed to variations small differences in the synchrony of cultures.

Figures 5(a)-(c) show the evolution of the optical properties during the stationary phase. As would be expected, due to the fact there is very little change in the biomass concentration, the optical properties show a much smaller variation compared to the growth phase. As in the case of the growth stage, the extracted optical properties are consistent over the three cultivations indicating the reliability of the inversion method. Figures 6(a)-(c) show the changes in the optical properties during the decline phase. The variations in the optical properties are smaller compared to the growth phase.

In order to have a closer look at the "direction" of variations in the optical properties over the course of a cultivation, the extracted values are plotted for two wavelengths 1050nm and 1602nm. These two wavelengths were chosen to examine the

behaviour of the optical properties in a scattering dominated region and an absorption dominated region respectively. In figure 7, the optical properties at 1050nm are plotted against the biomass concentration. It is seen from figure 7(a) that during the growth phase $\mu_s(\lambda)$ varies approximately linearly with the biomass except for one point with very low biomass concentration. This could due to the low biomass concentration resulting in a combination of measurement errors and the low scattering levels exacerbating errors in the inversion since the numerical method employed is based on multiple scattering effects being dominant. In the stationary phase, the bulk scattering coefficient does not show strong trends. This is due to the fact that the changes in biomass during this period are not large, trends if any will be swamped by the errors in the measurement of biomass. This characteristic is also seen in the decline phase. Overall, for the same levels of biomass, the values of $\mu_s(\lambda)$ in the decline phase are less than those observed in the stationary phase, possibly indicating differences in the biomass characteristics such as the morphology of viable and non-viable cells, clumping etc.

In the case of $\mu_a(\lambda)$ (Figure 7(b)), the relationship with biomass indicates a slight non-linearity with a curvature observable at the lower end (around the region of 0.5µg/ml) of the biomass concentration. Again samples at the lower cell densities are more likely to be outliers for reasons mentioned when discussing the bulk scattering coefficient in the last paragraph. The values of $\mu_a(\lambda)$ in the stationary and decline phase do not show any clear-cut clustering that was similar to that seen when examining $\mu_s(\lambda)$. This could be due to the lack of significant changes in the concentration of the cellular components over these periods.

The variation of the anisotropy factor $g(\lambda)$ with biomass is shown in figure 7(c). It is seen that during the growth phase, $g(\lambda)$ rises sharply and stabilises around 0.9 where it remains during the stationary phase. In the decline phase, $g(\lambda)$ takes on slightly lower values than observed for the stationary phase. The sharp increase in $g(\lambda)$ initially could be due to the rapid increase in rate of cell divisions creating a larger population of freshly divided cells (of smaller sizes) compared to the cells yet to divide into smaller cells. However, more investigation is needed to verify this explanation.

In figure 8, the optical properties at 1602nm are plotted against biomass concentration. The values for $g(\lambda)$ are not shown since, as discussed earlier, they were not reliable in this region. It is seen in figure 8(a), $\mu_s(\lambda)$ shows a non-linear relationship in contrast to the trend seen at 1050nm, remaining flat initially, and then rising rapidly with biomass concentration. There are two outliers observed in this region. These are more likely to be due to convergence problems in the inversion rather than to any physical characteristics in the system. As was the case for 1050nm, there are no discernible trends in the bulk scattering coefficient with respect to biomass in the stationary and the decline phase. Compared to the decline phase, $\mu_s(\lambda)$ appears to be slightly higher in the stationary phase. For the bulk absorption coefficient, it is seen that the relationship between $\mu_a(\lambda)$ and the biomass in the growth phase is weaker compared to that at 1050nm. Thus while the absorption and scattering properties change with the biomass concentration, the extent of this variation depends on wavelength.

CONCLUSIONS

This study shows that the absorption and scattering property changes during the cultivation of a bacterium can be consistently extracted from measurements under multiple scattering conditions. The cultivation system considered here was a simple one where the major change during the cultivation process was the increase in biomass. This is reflected by the fact that the greatest relative change was seen in the scattering properties during the growth phase. Since the wavelength range used in this study (950-1850nm) spans two different regimes viz. the absorption dominated and scattering dominated regions, the path length of the cuvette used may not be optimal for extracting the optical properties with sufficient accuracy over the entire wavelength range. The extreme example occurs around the water peak at the 1400-1500nm region. In the context of using this approach to separate absorption and scattering effects so that effective models can be built for monitoring concentrations of nutrients, biomass etc., further studies have to be conducted to establish the effect of sample thickness on the extracted optical properties. We also have to determine how reliable the extraction method will be at higher biomass concentrations i.e. at levels which are usually encountered in industrial situations. This is because at high biomass concentrations the collimated transmittance signal will be adversely affected. This issue has to be successfully overcome for this approach to be used as a means of correcting scattering effects when building calibration models for estimating concentrations of (e.g. glucose, product etc) analytes.

ACKNOWLEDGMENTS

This work was funded by Marie Curie FP6 (INTROSPECT) and by EPSRC grants GR/S50441/01 and GR/S50458/01.

References

1. S. A. Arnold, J. Crowley, S. Vaidyanathan, L. Matheson, P. Mohan, J. W. Hall, L. M. Harvey, and B. McNeil, Enzyme and Microbial Technology **27**, 9, 691 (2000).

2. S. Vaidyanathan, G. Macaloney, J. Vaughn, B. McNeil, and L. Harvey, Critical Reviews in Biotechnology **19**, 4, 277 (1999).

3. D. Cozzolino, R. Dambergs, L. Janik, W. Cynkar, and M. Gishen, Journal of Near Infrared Spectroscopy **14**, 5, 279 (2006).

4. S. Engelhard, M. U. Kumke, and H. G. Lohmannsroben, Analytical and Bioanalytical Chemistry **384**, 5, 1107 (2006).

5. S. A. Arnold, L. M. Harvey, B. McNeil, and J. W. Hall, Biopharm International-the Applied Technologies of Biopharmaceutical Development **15**, 11, 26 (2002).

6. S. A. Arnold, L. M. Harvey, B. McNeil, and J. W. Hall, Biopharm International-the Applied Technologies of Biopharmaceutical Development **16**, 1, 47 (2003).

7. S. Rathore, M. Paulsen, V. Sharma, and V. Singh, "Near-Infrared Spectra Interpretation of Fermentation in a Dry Grind Corn Process", in *ASAE Annual Internationa Meeting* (Tampa Convention Center, Tampa, Florida, 2005).

8. M. Scarf, A. Arnold, L. Harvey, and B. McNeil, Critical Reviews in Biotechnology **26**, 1, 17 (2006).

9. A. Ishimaru, *Wave Propagation and Scattering in Random Media* (IEEE Press, Oxford University Press, 1997).

10. K. N. Liou, *An Introduction to Atmospheric Sciences*, (Academic Press, San Diego, California USA, 2002).

11. S. A. Prahl, "The Adding-Doubling Method," in *Optical Thermal Response of Laser Irradiated Tissue*, A. J. Welch, and v. G. M. J. C., eds. Plenum Press, New York, (1995),pp. 101–129.

12. W. Saeys, M. Velazco-Roa, S. Thennadil, H. Ramon, and B. Nikolai, Applied Optics **47**, 7, 908 (2008).

13. M. A. Velazco-Roa and S. N. Thennadil, Applied Optics **46**, 18, 3730 (2007).

14. W. J. Wiscombe, J. Quant. Spectrosc. Radiat. Transfer **16**, 637 (1976).

15. C. R. Harwood and S. M. Cutting, *Molecular Biology Methods for Bacillus* (John Wiley & Sons Ltd., 1990).

LIST OF FIGURES

Figure 7 Estimated optical properties at 1050nm during growth, stationary and decline phase for 3 cultivations (grey symbols-growth phase, solid black symbols-stationary phase, open symbols-decline phase) versus biomass. (a) Scattering coefficient μ_s, (b) Absorption coefficient μ_a and (c) Anisotropy factor g.

Figure 8 Optical properties at 1602nm during growth, stationary and decline phase for 3 cultivations (grey symbols-growth phase, solid black symbols-stationary phase, open symbols-decline phase) versus biomass. (a) Scattering coefficient μ_s, (b) Absorption coefficient μ_a.

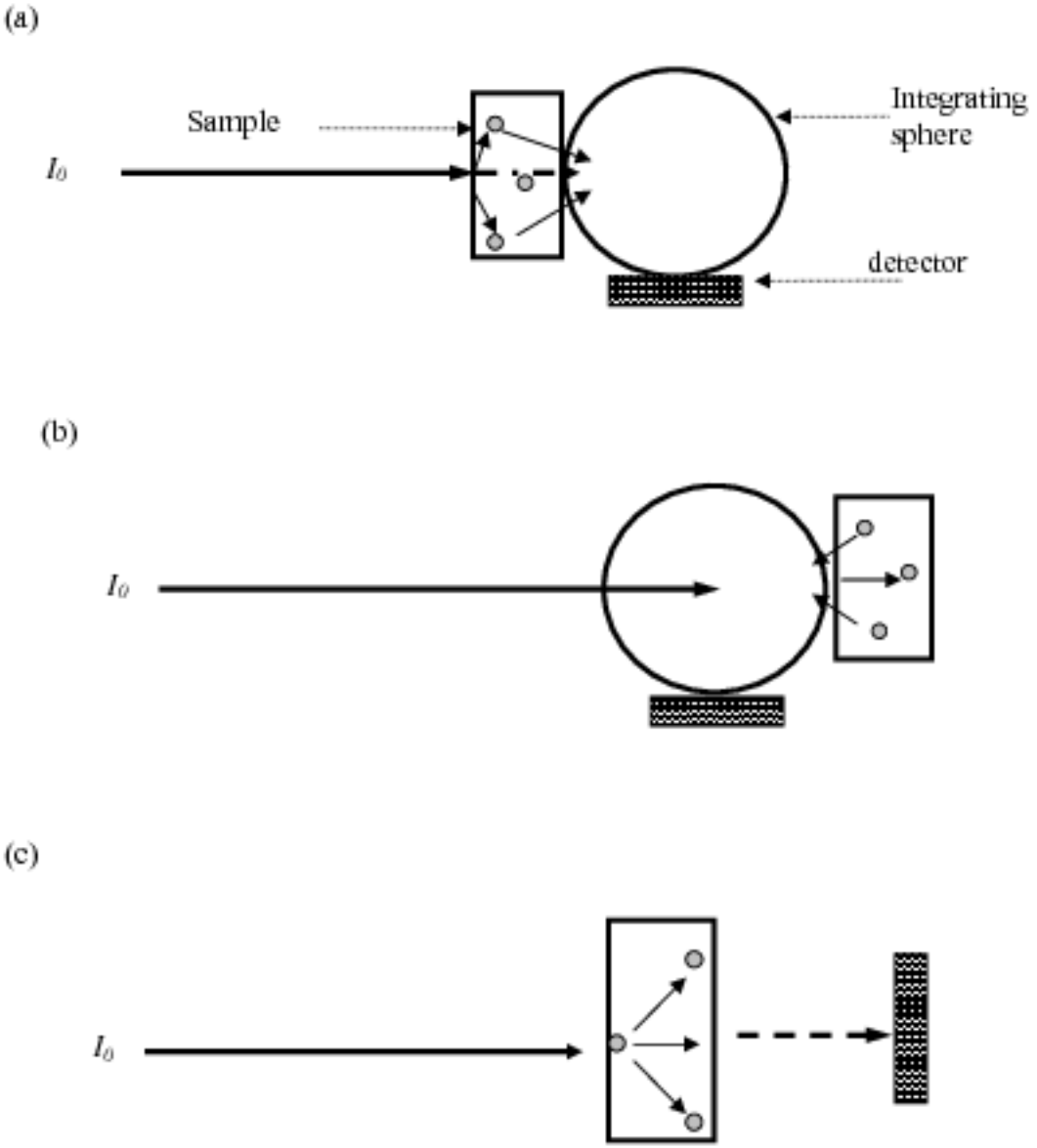

Figure 1 Experimental setup for measuring (a) Total Diffuse Transmittance (b) Total Diffuse Reflectance, and (c) Collimated Transmittance T_c.

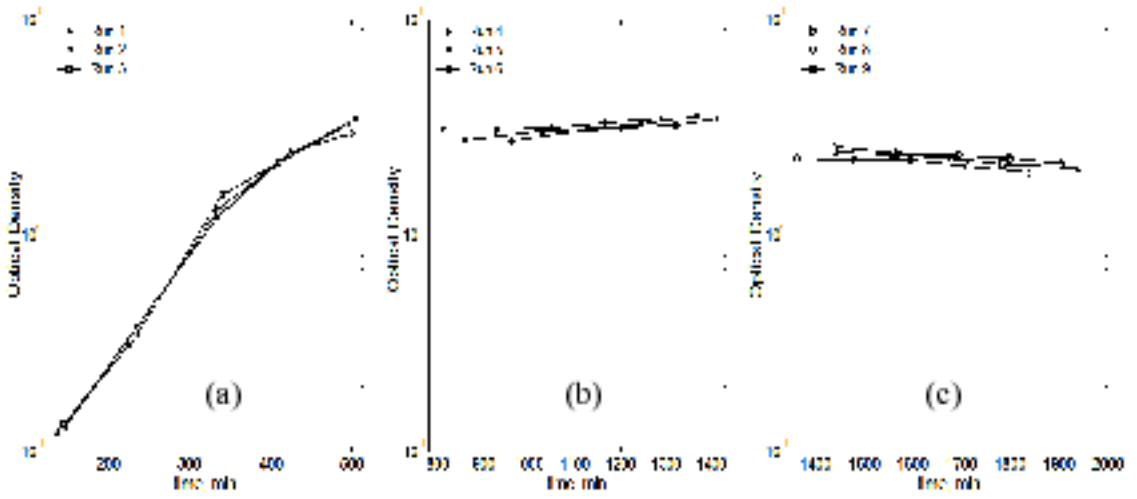

Figure 2 *Bacillus subtilis* growth profiles for three cultivations: (a) the growth phase, (b) stationary phase and (c) decline phase.

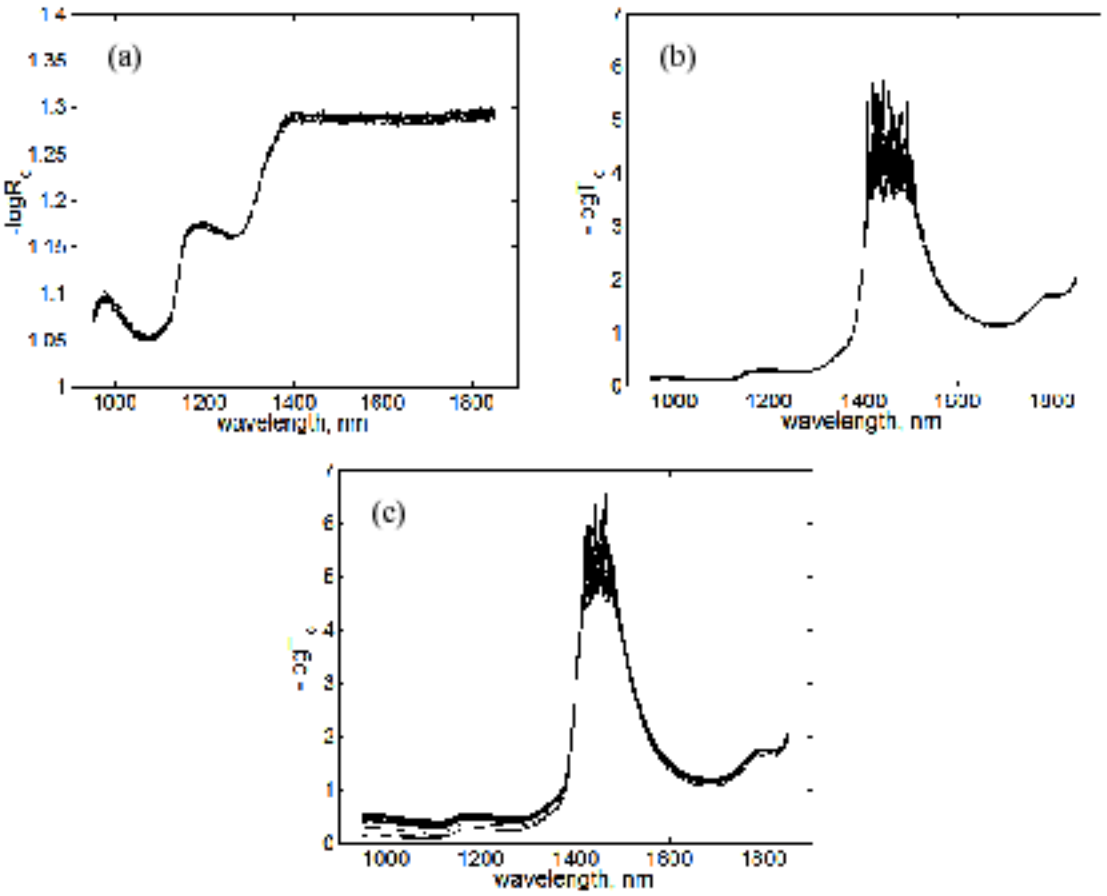

Figure 3 Spectra of samples taken at different stages of the growth cycle (growth phase, stationary phase, decline phase). (a) Total diffuse reflectance, (b) Total diffuse transmittance and (c) Collimated transmittance.

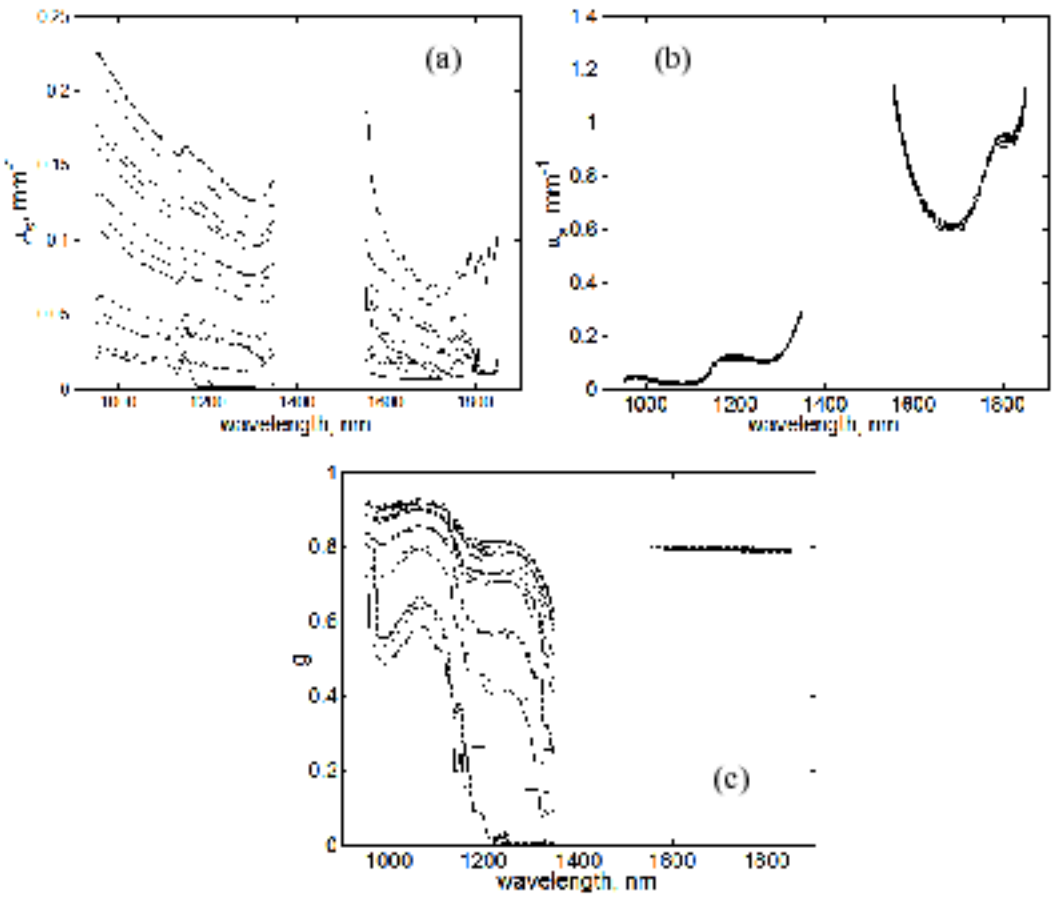

Figure 4 Estimated optical properties and anisotropy factor during growth phase for 3 cultivations (Solid line-Run 1, Dashed line-Run 2, Dotted line -Run 3). (a) Scattering coefficient μ_s, (b) Absorption coefficient μ_a and (c) Anisotropy factor g.

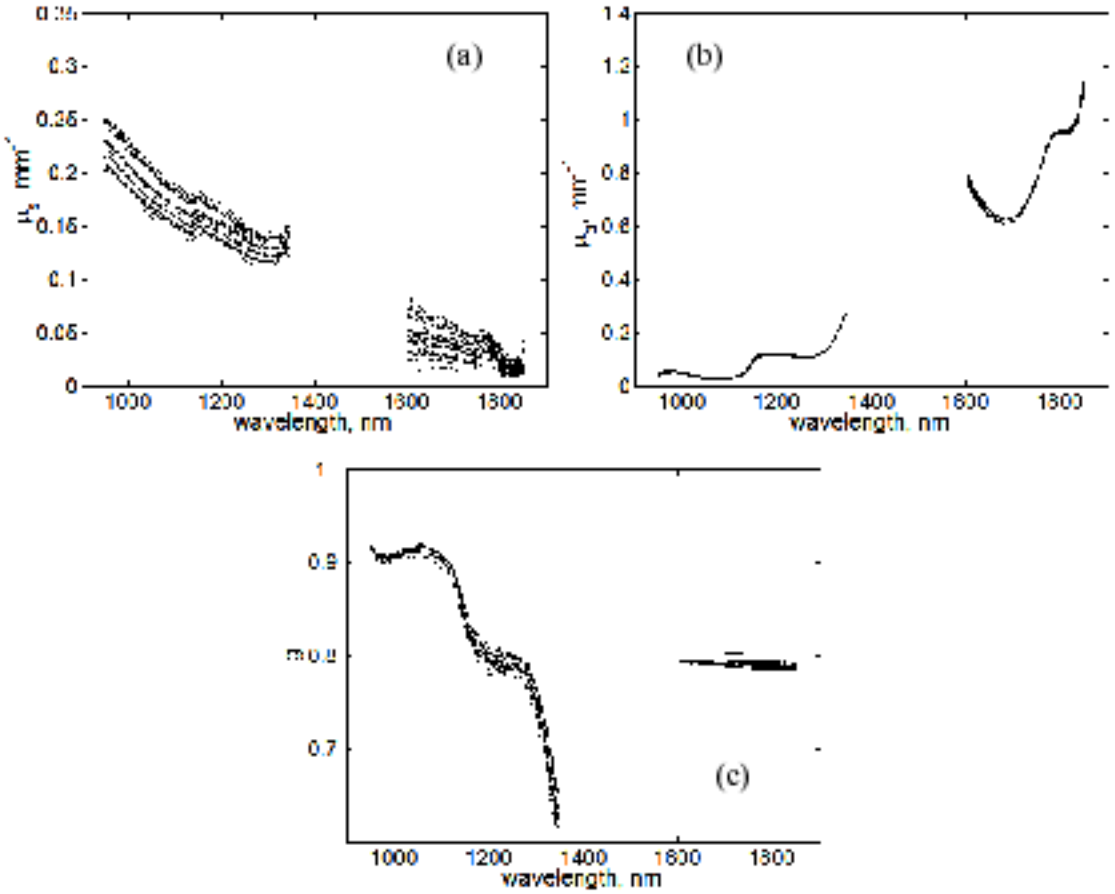

Figure 5 Optical properties during stationary phase for 3 cultivations (Solid line-Run 4, Dashed line-Run 5, Dotted line - Run 6). (a) Scattering coefficient μ_s, (b) Absorption coefficient μ_a and (c) Anisotropy factor g.

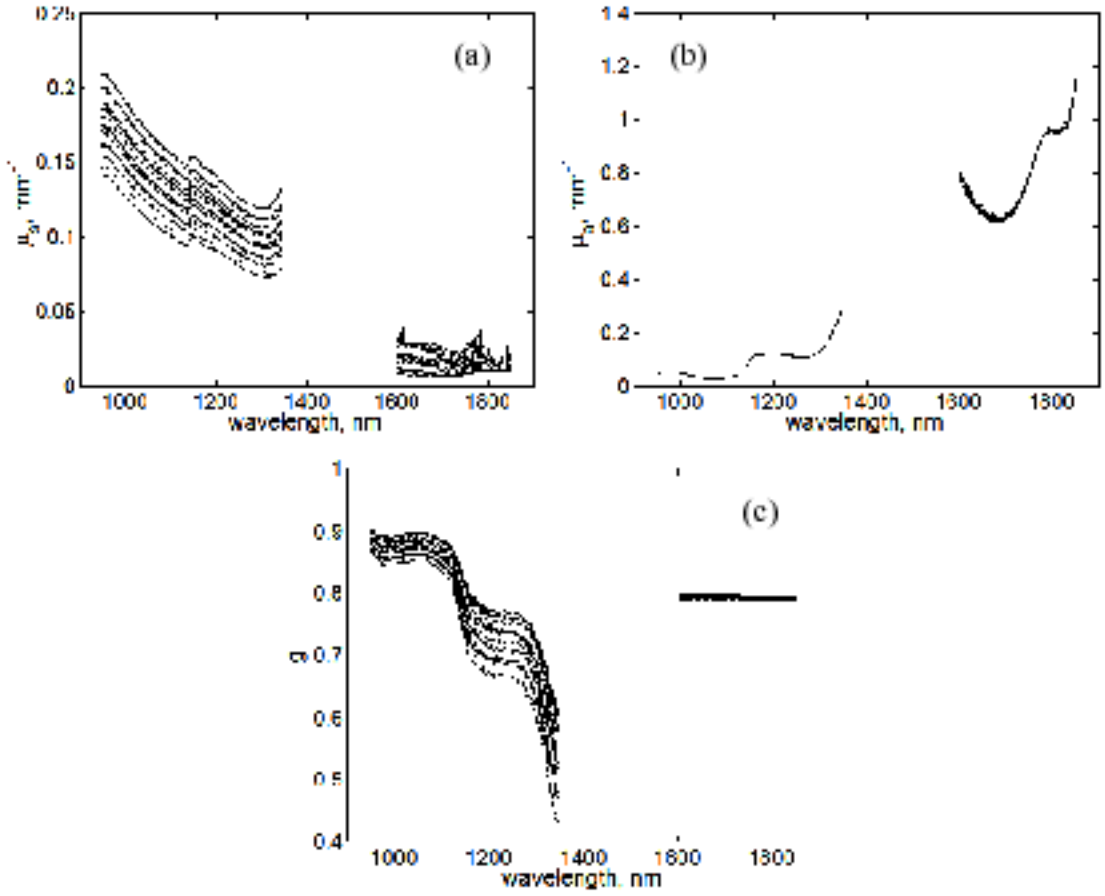

Figure 6 Estimated optical properties and anisotropy factor during decline phase for 3 cultivations (Solid line-Run 7, Dashed line-Run 8, Dotted line - Run 9). (a) Scattering coefficient μ_s, (b) Absorption coefficient μ_a and (c) Anisotropy factor g.

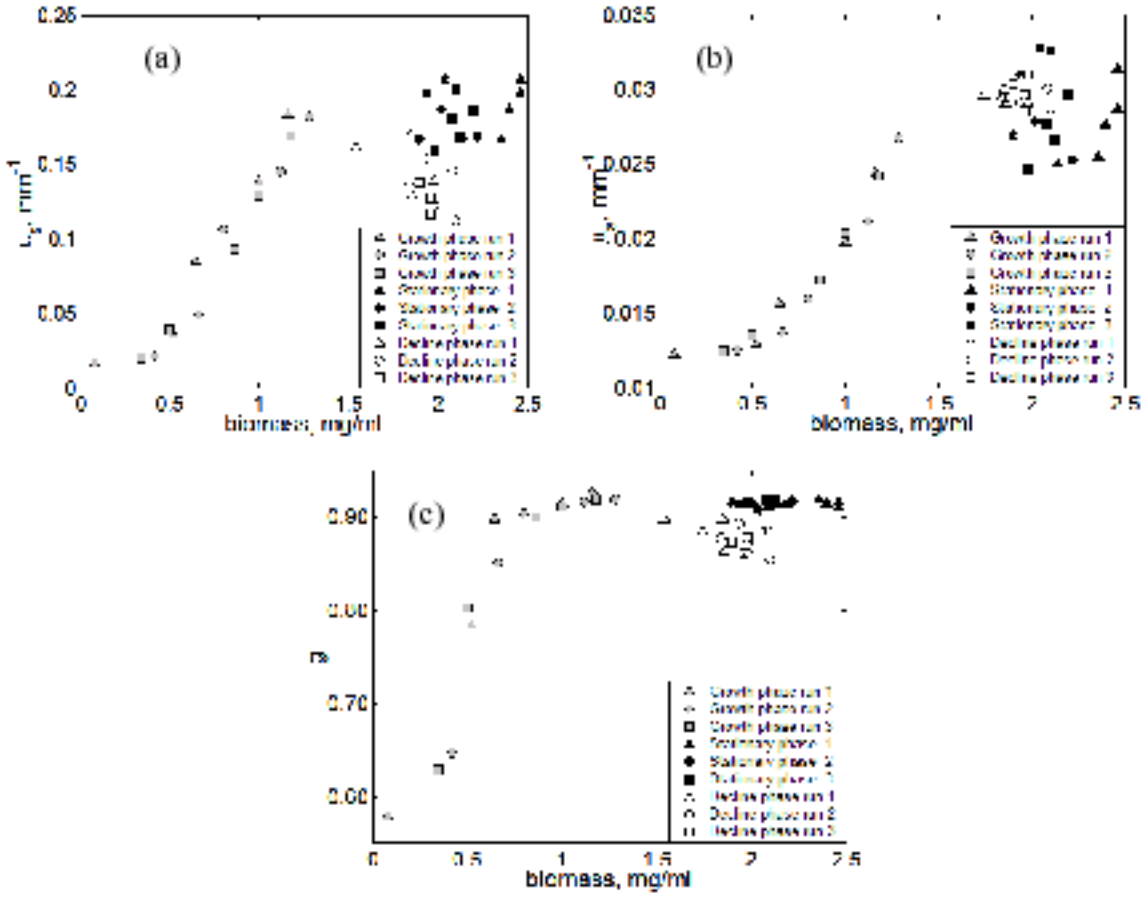

Figure 7 Estimated optical properties at 1050nm during growth, stationary and decline phase for 3 cultivations (grey symbols-growth phase, solid black symbols-stationary phase, open symbols-decline phase) versus biomass. (a) Scattering coefficient μ_s, (b) Absorption coefficient μ_a and (c) Anisotropy factor g.

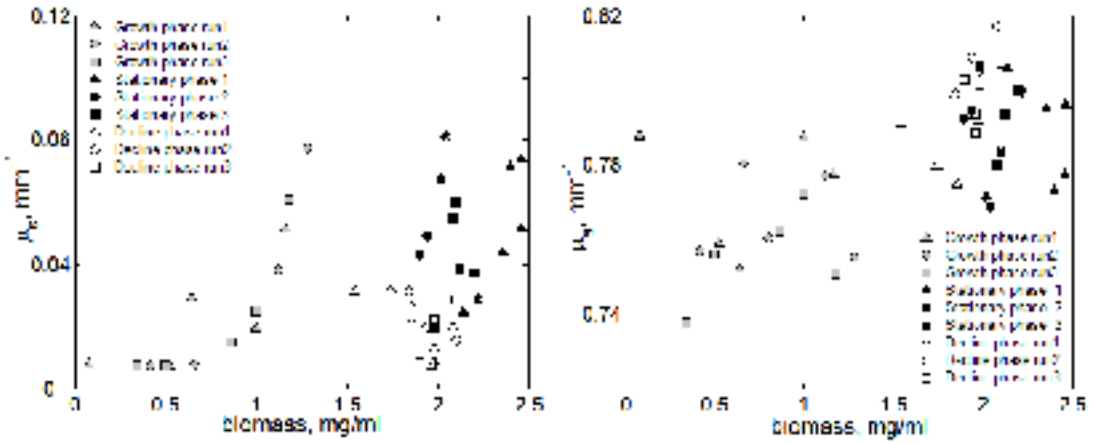

Figure 8 Optical properties at 1602nm during growth, stationary and decline phase for 3 cultivations (grey symbols-growth phase, solid black symbols-stationary phase, open symbols-decline phase) versus biomass. (a) Scattering coefficient μ_s, (b) Absorption coefficient μ_a.